

Enhanced catalytic activity of enzymes interacted with nanometric titanate nanosheets

Kai Kamada,^{a,*} Akane Yamada^a and Nobuaki Soh^b

Received 00th January 20xx,
Accepted 00th January 20xx

DOI: 10.1039/x0xx00000x

www.rsc.org/

Coexistence effect of titanate nanosheets (TNS) with nanometric lateral dimensions (ca. 3 nm), which were prepared through a hydrolysis reaction of titanium tetraisopropoxide, on catalytic activity of horseradish peroxidase (HRP) was investigated as a function of solution pH. Especially in diluted HRP solutions with a pH range of 7 ~ 8, enzymatic reaction rate, i.e., maximum velocity (V_{max}) in the conventional Michaelis-Menten equation, was significantly enhanced more than 2 times in the presence of TNS. In contrast, the increase in V_{max} was not very large in acidic (pH = 4.0) and basic solutions (pH = 9.0). It was demonstrated that the TNS brought about peptization of aggregates composed of several HRP molecules in a diluted solution, causing increase in an apparent HRP concentration participating in the enzymatic reaction. Moreover, the coexistent TNS activated superoxide dismutase (SOD) with O_2^- scavenging performance.

Introduction

As well-known, enzymes are biocatalysts with excellent substrate specificity and reaction route selectivity. In addition, since catalytic reactions with enzymes proceed even at moderate temperature, various kinds of enzymes have been utilized in numerous industrial applications including chemical manufacturing and pollutant purifications. In practical application, to enhance physicochemical stability in non-physiological conditions, enzymes have been frequently immobilized on stable solid surface of oxides¹ and polymers,² and such hybrid materials are recognized as “immobilized enzymes”. One advantage of immobilized enzymes is that tiny enzyme molecules are easily recovered from a reaction system then reused many times.³ In general, stability of an enzyme is reinforced in proportion to binding energy to a solid support.⁴ Although thermal or chemical durability of immobilized enzymes is surely reinforced, an apparent enzymatic activity at an ambient atmosphere is reduced because the binding to a solid support prohibits Brownian motion of enzyme molecules in a solvent, causing deterioration in accessibility to external substrate molecules.

So far, several kinds of oxide, hydroxide or phosphate nanosheets have been employed for immobilization of enzymes,⁵⁻⁸ and stability improvements at high temperature⁹ or in non-aqueous medium⁹ have been accomplished. In these cases, enzymes are sandwiched between nanosheets. Titanate nanosheets (called below as TNS) have been used most frequently because of high chemical stability, a well-

established synthesis technique, etc.^{10,11} Other literatures have proved that catalytic activity of enzymes bound to inorganic host nanomaterials including TNS can be manipulated by photo-irradiation with enough energy to excite the hosts followed by thermal energy or photocarrier transfer to the enzymes.¹²⁻¹⁶ As an analogous approach, Kragl and coworkers have reported enzymatic activity control with a laser-light-induced pH change of a solution including photo-dissociative carboxylates.^{17,18} Intercalation of enzymes into nanosheets has an analogous problem with conventional immobilized enzymes. That is, catalytic activity of enzymes in interlayer space decreases under an ambient condition,¹⁹ because only enzymes exposed near or adsorbed on the surface can participate in a reaction. In other words, substrates cannot approach to enzymes deeply inserted inside the interlayer space. This is caused by a large discrepancy between two-dimensional (lateral) sizes of the nanosheets ($\sim 10^4$ nm) and molecular dimensions of enzymes (typically less than 10 nm). As a rare example, Kumar et al. have reported that enzymatic (enzyme mimetic) activities including peroxidase-like activity of heme proteins are improved by hybridizing with negatively charged zirconium phosphate (α -ZrP) nanosheets only for limited substrates.^{20,21} They discussed effects of an oxidation potential and molecular conformation of substrate on the variation in activity. Besides inorganic nanosheets, enhanced performance of laccase bound to phosphate functionalized carbon dots has been clarified by Kang and coworkers.^{22,23} In this case, surface functional groups of carbon dots attract substrates near to the simultaneously bound laccase.

In the present study, we report that binding of oxidoreductase (horseradish peroxidase, HRP) to TNS with nanometric lateral dimensions less than 10 nm drastically increases an enzymatic reaction rate. The TNS were mixed with an HRP solution at various pH values, and then enzymatic

^a Department of Chemistry and Materials Engineering, Graduate School of Engineering, Nagasaki University, Nagasaki 852-8521, Japan. Email: kkamada@nagasaki-u.ac.jp

^b Faculty of Agriculture, Saga University, Saga 840-8502, Japan.

activity was evaluated by using 2-methoxyphenol (guaiacol) as a substrate to be oxidized. It was verified that the HRP was highly activated in the presence of TNS. Such favorite phenomenon was explained on the basis of a physicochemical interaction between TNS and HRP. This desirable change is due to a novel mechanism completely different from the aforementioned literatures, i.e., “well dispersion stability of enzymes bound to TNS”. As well as HRP, the elevated activity by connecting with TNS is also confirmed for another enzyme (superoxide dismutase).

Experimental

A colloidal solution of TNS was fabricated through a hydrolysis reaction of pure titanium tetraisopropoxide liquid (99.999%) with a tetrabutylammonium (TBA⁺) hydroxide solution,²⁴ where a molar ratio of TBA⁺ for Ti was set to unity. After the hydrolysis at room temperature, the mixture was aged at 60°C for 2 h with vigorous shaking followed by a dialysis to remove by-products such as isopropanol and excess TBA⁺ ions. Deionized water was added to the concentrated colloidal solution and then the dialysis was conducted again. The procedure was repeated to obtain a neutral colloidal solution of TNS (pH ~ 8). The crystal structure of TNS was analyzed by X-ray diffraction (XRD) after drying the colloidal solution on a glass plate. The particle size of TNS a two-dimensional anisotropy in shape was evaluated by dynamic light scattering (DLS) measurement on assumption that the particle had a spherical morphology.

To investigate an effect of TNS on enzymatic activity of HRP, the TNS colloidal solution ([Ti] = 13.7 mM, 0.120 mL) were added to peroxidase (horseradish peroxidase (HRP), MW: 44,000) dissolved in 20 mM buffer solutions ($m_{\text{HRP}} = 5 \mu\text{g/ml}$, 0.120 mL) with several pH values (4.0 (acetate), 7.0, 8.0, 8.5, and 9.0 (tris-HCl)) in a transparent polystyrene cuvette, then the mixtures were gently shaken for 30 min at room temperature. The enzymatic activity of HRP was measured using an oxidation of 2-methoxyphenol as a substrate in a buffer solution with an identical pH to the mixture of HRP and TNS. A 100 mM buffer solution (1.872 mL) was added to the cuvette containing the mixed HRP-TNS solution. The enzymatic reaction rate was calculated from an initial linear increase in absorbance at $\lambda = 470 \text{ nm}$ (A_{470}) immediately after injection of an aqueous solution of 135 mM H_2O_2 (0.048 mL, 2.7 mM in the final concentration), because a polymeric oxidation product of 2-methoxyphenol has a maximum optical absorption at the wavelength (molar absorption coefficient: 26.6 cm²/mM). The measurement of A_{470} was undertaken at a constant temperature of 298 K under stirring by using a UV-Vis spectrophotometer. The enzymatic reaction rate was repeatedly measured under different concentrations of 2-methoxyphenol up to 40 mM, while the H_2O_2 concentration was fixed to 2.7 mM. An enzymatic activity of free HRP was also evaluated as a control using the same method except for using deionized water in place of the TNS colloidal solution.

An effect of the TNS on activity was also studied for another enzyme, superoxide dismutase (SOD), which catalyzes

dismutation of superoxide anion radicals (O_2^-) to O_2 and H_2O_2 . The TNS colloidal solution was added to an SOD solution in the ratio of Ti/SOD = 6.54 pmol/U. O_2^- radicals were generated using a hypoxanthine (HX) / xanthine oxidase (XOD) reaction system. Coexistent cytochrome c is reduced by the O_2^- and then gives rise to a rapid increment of absorbance at 550 nm (A_{550}). Therefore, variation in A_{550} after injection of 0.72 mM HX (30 μL) to mixed solution of enzyme (free SOD or SOD-TNS, 15 μL), XOD (30 mU/mL, 30 μL), and cytochrome c (3 mg/mL, 3 μL) in 20 mM tris-HCl buffer solution dissolving 1 mM EDTA (pH = 9.0, 237 μL) was recorded using a microplate reader for 3 min at 310 K, where the measurement was carried out in a well of a 96-well transparent microplate. Taking into account a linear proportion of initial slope of A_{550} to the O_2^- concentration, the O_2^- scavenging activity of SOD or SOD-TNS was defined as a decreasing ratio of the slope for the enzyme-free solution. The identical measurement was repeated three times and average values were used to draw a dose-dependent annihilation curve of SOD and SOD-TNS.

Results and Discussion

The hydrolysis of titanium tetraisopropoxide with a tetrabutylammonium (TBA⁺) hydroxide solution and the subsequent dialysis resulted in formation of colorless and transparent solution. The obtained solution clearly scatters a beam of laser light, meaning existence of tiny solid particles. Particle size distribution of the colloidal solution measured by a dynamic light scattering method was given in Fig. 1a as “TNS”. The mean particle size was estimated to be ca. 3 nm.

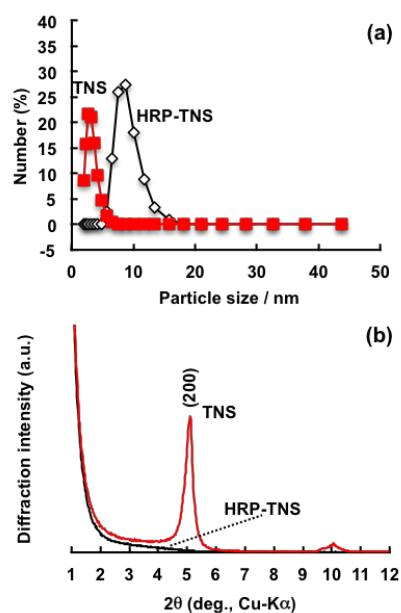


Fig. 1. (a) Particle size distribution curves of colloidal solution of TNS ([Ti] = 13.74 mM) and a 0.1 M tris-HCl buffer solution (pH = 8.0) including HRP (20 $\mu\text{g/ml}$) and TNS ([Ti] = 0.07 mM) denoted as HRP-TNS. (b) XRD patterns of a TNS colloidal solution after drying on a glass plate and HRP-TNS particles produced at pH = 4.0.

This reveals that the colloidal particles have comparable dimensions to an HRP (3.0*3.5*6.0 nm). In other words, the

TNS have nanometric lateral dimensions in contrast that most TNS employed previously have been a few μm .¹⁹ The X-ray diffraction pattern of the colloidal solution after drying on a glass plate was measured and the result was included in Fig. 1b. According to literatures,^{24,25} the colloidal particles prepared by the present hydrolysis technique have a crystal structure consisting of tetratitanate ($\text{Ti}_4\text{O}_9^{2-}$). In fact, the diffraction line assigned to a (200) crystal plane of $\text{Ti}_4\text{O}_9^{2-}$ nanosheets inserting counter TBA^+ ions was discernible.

Fig. 2 plots oxidation velocities (V) catalyzed by HRP (0.25 $\mu\text{g}/\text{ml}$) in the presence or absence of TNS as a function of substrate (2-methoxyphenol) concentration at $\text{pH} = 8.0$. Irrespective of the coexistence of TNS, the V was increased with increasing the substrate concentration and then saturated at a high concentration in obedience to the conventional Michaelis-Menten equation. The kinetic parameters (Michaelis constant; K_m and maximum reaction velocity; V_{max}) were determined by a non-linear curve fitting of the V against the substrate concentration. The resultant fitting curves are drawn as solid lines in Fig. 2. At $\text{pH} = 8.0$, the maximum velocity (V_{max}) of HRP-TNS was $1.24 \mu\text{M}\text{s}^{-1}$, whereas that of free HRP was $0.57 \mu\text{M}\text{s}^{-1}$. Namely, the addition of TNS raised the V_{max} more than double, in contrast that binding of HRP to TNS with large lateral dimensions ($\sim 10 \mu\text{m}$) considerably reduced enzymatic activity as reported in our previous papers.^{10,14} Furthermore, the slightly lower K_m for HRP-TNS could be related to an improved substrate affinity for HRP. On the other hand, no change in absorbance at 470 nm was observed for a 2-methoxyphenol solution including the TNS only, indicating that the TNS had no enzyme-mimetic activity. Judging from these findings, the activity enhancement in Fig. 2 should be based on some interaction between HRP and TNS.

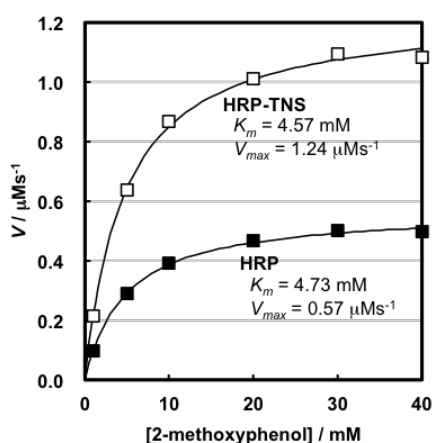


Fig. 2 Dependence of substrate (2-methoxyphenol) concentration on enzymatic oxidation velocity (V) of free HRP and HRP-TNS at $\text{pH} = 8.0$ and 298 K.

Table 1 Kinetic parameters of enzymatic oxidation of 2-methoxyphenol using free HRP and HRP-TNS at 298 K.

pH	$V_{max} / \mu\text{M}\text{s}^{-1}$		Relative V_{max}	K_m / mM		Relative K_m
	HRP	HRP-TNS		HRP	HRP-TNS	
4.0	0.33	0.34	1.03	5.71	4.48	0.78
7.0	0.71	1.76	2.48	2.07	2.06	0.99
8.0 ^a	0.57	1.24	2.17	4.73	4.57	0.97
8.5	0.57	0.71	1.24	6.22	5.34	0.86
9.0	0.67	0.75	1.12	20.97	19.44	0.93

^aThe standard deviations ($n = 4$) of V_{max} of free HRP and HRP-TNS at $\text{pH} = 8.0$ were 0.01 and less than $0.01 \mu\text{M}\text{s}^{-1}$ and those of K_m were 0.25 and 0.30 mM, respectively.

Table 1 summarizes estimated kinetic parameters of free HRP and HRP-TNS for oxidation of 2-methoxyphenol under various pH values. As expected, a free HRP showed a relatively high maximum reaction velocities V_{max} at $\text{pH} = 7.0 \sim 9.0$, while the V_{max} was dramatically reduced in an acidic solution ($\text{pH} = 4.0$). The K_m value was extremely large only at $\text{pH} = 9.0$. This may be concerned with electrostatic repulsion between negative TNS and anionized substrates (dissociation of phenolic OH groups) because the $\text{p}K_a$ of 2-methoxyphenol has been reported to be 9.93.²⁶ In this case, a percentage of dissociated substrates were calculated to be ca. 11 mol% at $\text{pH} = 9.0$.

In the case of HRP-TNS, on the other hand, the V_{max} was distinctly maximized at $\text{pH} = 7.0$. To reveal the effect of TNS addition on the catalytic activity of HRP, relative ratios of V_{max} and K_m of HRP-TNS against those of free HRP were plotted as a function of pH (Fig. 3). The V_{max} ratios exceed unity at all pH values employed in the present study, suggesting that the HRP-TNS possesses a relatively high enzymatic activity over a wide range of pH. Especially, it should be noted that the V_{max} at $\text{pH} = 7.0$ is about 2.5 times greater than that of free HRP. Within our knowledge, the extent of enhancement is largest ever along with catalytic oxidation of 4-methoxyphenol by HRP intercalated into α -ZrP layered structure.²⁰ Moreover, the similar preferable effect has been confirmed for other substrates including a luminol,²⁷ that is, the TNS addition is effective for various substrates unlike α -ZrP with considerable substrate dependence. Focusing on the K_m ratios, although there is little noteworthy trend, all values are less than unity, meaning an improved affinity of 2-methoxyphenol for HRP under the existence of TNS.

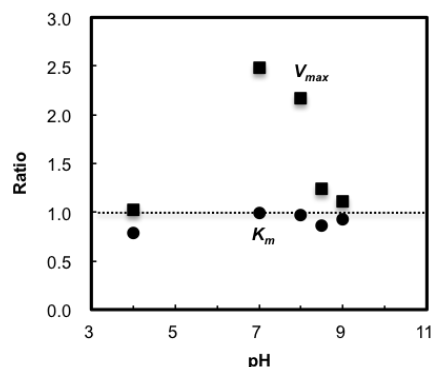


Fig. 3 pH dependence of K_m and V_{max} ratio of HRP-TNS against those of free HRP.

To clarify the mechanism of the activity enhancement, concentration dependence of an HRP size distribution in 0.1 M tris-HCl buffer solution (pH = 8.0) was assessed by means of the DLS method. Fig. 4a and b display size distribution curves of HRP and mean sizes in solutions with different HRP concentrations, respectively. The distribution curves at high HRP concentrations of 100 $\mu\text{g}/\text{ml}$ and over are composed of a single peak, which is located around the reported dimensions of an HRP molecule (~ 6.0 nm), indicating most HRP molecules exist as a single molecule. It should be noted that an additional broad peak with a larger size appears in the diluted HRP solutions less than 100 $\mu\text{g}/\text{ml}$. The fact implies that HRP molecules partially agglomerate to form large aggregates that increase the mean size significantly as seen in Fig. 4b. Unfortunately, the DLS measurement at a low concentration used for the activity evaluation (0.25 $\mu\text{g}/\text{ml}$) was impossible because of extremely weak laser light scattering intensity. However, it is believed that the aggregation of HRP also occurs in such a highly diluted solution.^{27,28} The expectation is supported by the experimental findings that the kinetic parameters of HRP-TNS ($V_{\text{max}} = 2.47 \mu\text{Ms}^{-1}$, $K_m = 0.97 \text{ mM}$) were almost equal to those of free HRP ($V_{\text{max}} = 2.53 \mu\text{Ms}^{-1}$, $K_m = 1.14 \text{ mM}$) at a high HRP concentration (0.5 $\mu\text{g}/\text{ml}$). Fig. 1a includes the particle size distribution curve of HRP (20 $\mu\text{g}/\text{ml}$) after mixing with the TNS, and the calculated average size was displayed as an open circle in Fig. 4b. These data evidently suggest that the peak attributed to the HRP aggregation completely disappeared and the apparent molecular size of HRP was reduced by the coexistence of TNS. That is, the HRP aggregates were dissociated to single molecules. Considering these evidences along with the tiny reduction in the K_m , the activity enhancement of HRP may be due to an increase in an effective concentration of HRP by peptizing the HRP aggregates in the presence of TNS.

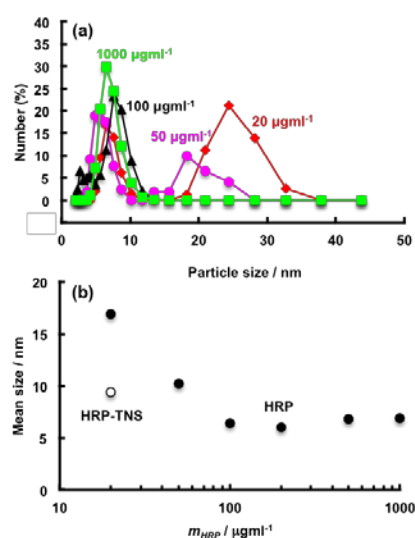


Fig. 4 (a) Size distribution curves of HRP with different concentrations in 20 mM tris-HCl buffer solution at pH = 8.0. (b) Effect of concentration on apparent mean size of HRP accompanied by 20 $\mu\text{g}/\text{ml}$ HRP hybridized with the identical weight of TNS.

In general, an electrostatic interaction has been frequently utilized for intercalation of enzymes into nanosheets in an aqueous solution. When they have an opposite sign of surface charge at a specific pH, spontaneous bond formation between them takes place. It is well-known that a sign and magnitude of surface charge can be manipulated by adjusting a solution pH. According to our previous papers,¹⁹ it was revealed that an isoelectric point (pI) of HRP and TNS was 5 and 2, respectively. This fact implies that a “tight” electrostatic interaction is generated to form HRP-TNS hybrids at a range of $2 < \text{pH} < 5$, because negatively charged TNS firmly attract HRP with a positive charge. However, it should be noted that the elevated activity of HRP was found out of the pH range ($\text{pH} = 7.0 \sim 8.0$) and little activity change was observed inside the range ($\text{pH} = 4.0$). As stated above, the peptization of HRP by TNS would play a key role for the significantly enhanced activity more than 2 times at neutral pH solutions. Even though both components have a negative net charge in the neutral solutions, a weak local interaction will be produced in inter-macromolecules such as TNS and HRP. More concretely, negatively ionized carboxyl and positively ionized amino groups of amino acid residues in an HRP surface are interacted with hydrogen and oxygen of surface hydroxyl groups of TNS, which is agreed with formation of hydrogen bonds. This expectation is supported by the fact that dissociation constants (pK_a) of $-\text{COOH}$ and $-\text{NH}_3^+$ in a multitude of amino acids are distributed around 2 and 10, respectively, meaning most amino acid residues possess as $-\text{COO}^-$ or $-\text{NH}_3^+$ in the pH range handled in the present study. Furthermore, tetrabutylammonium ions (TBA^+) existing as a counter ion could adsorb on the negative TNS surface, then produce an electric double layer. The HRP molecules might be connected to the TNS via the TBA^+ ion adsorbed (ion-coupled bonding).⁵ When the total of these interactions is greater than cohesive force among HRP molecules, HRP aggregates are peptized and stabilized as single molecules. As a result, an effective concentration of HRP was increased, and then resulted in the largely enhanced V_{max} and the minor reduction in K_m .

In the pH dependence of relative V_{max} ratio (Fig. 3), the deterioration in the ratios above $\text{pH} = 8.0$ could be governed by increasing total negative charge density of TNS and HRP, that weakened the peptization effect of TNS. On the other hand, at $\text{pH} = 4.0$, TNS and HRP had an aforementioned firm interaction and produced huge aggregates that could be discernible in naked eyes. The XRD pattern of the aggregates after lyophilization is shown in Fig. 1b (HRP-TNS). In the previous literatures,^{9,10} intercalation of enzyme molecules into large inorganic nanosheets with a few μm in a two-dimensional size resulted in an appearance of diffraction lines attributed to expanded interlayer space by inserting larger enzymes than original inorganic ions. This meant interlayer enzymes and nanosheets are periodically arranged. In Fig. 1b, in contrast, no diffraction line was observed in the pattern, suggesting that the aggregates would consist of disordered arrangement of HRP and TNS. The HRP existing inside the huge aggregates could be difficult to give rise to the enzymatic reaction, and hence the effect of addition of TNS merely

appeared at pH = 4.0. Taken these findings together, the volcano-shaped pH dependence of V_{max} ratio described in Fig. 3 can be understandable.

Effect of the weak interaction between HRP and TNS on chemical stability of HRP was evaluated at pH = 8.0, where a small amount of ethanol (5 vol%) was mixed to the reactant solution in order to accelerate denaturation of HRP. Variations in activity retention% of free HRP and HRP-TNS at 298 K showed that both materials have a similar trend, that is, the enzymatic activities were gradually decreased with increasing the aging time (retention of ca. 80% after 8 h). This implies the “weak” interaction was invalid for stability enhancement of HRP and the “tight” electrostatic interaction is required to improve thermal and/or chemical stability.

Considering the activity enhancement mechanism discussed here, the TNS addition should be useful for other enzymes. Hence, the TNS was mixed with superoxide dismutase (SOD), which catalytically disproportionates superoxide anion radicals (O_2^-), then annihilation activity of O_2^- was evaluated. Fig. 5 indicates dose-dependent O_2^- annihilation curves of free SOD and SOD-TNS. These curves could be approximated by the typical sigmoid-function and a 50% inhibitory concentration of O_2^- (IC_{50}) of SOD was calculated.^{29,30} The IC_{50} of SOD was successfully reduced from 0.170 to 0.036 U in the presence of TNS. The annihilation ability of SOD was elevated especially at low SOD concentrations less than 1 U. This is consistent with the fact that the TNS addition was prominent in a diluted solution of enzyme. The result revealed that the positive effect of TNS was effective for other enzymes as well as HRP.

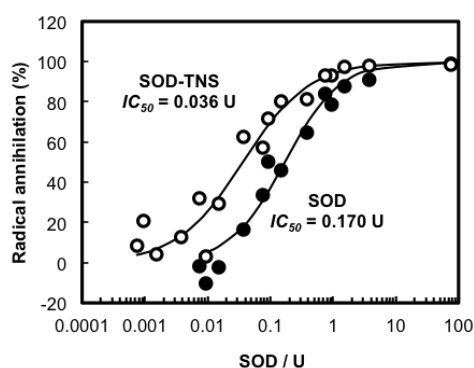


Fig. 5 Dose-dependent annihilation curves of SOD and SOD-TNS at pH = 9.0.

Conclusions

The present study investigated effect of presence of titanate nanosheets (TNS) on catalytic activity of horseradish peroxidase (HRP). In neutral and diluted HRP solutions, the coexistence of TNS significantly stimulated an enzymatic reaction rate more than 2 times. The favorable influence of TNS was explained by a change in dispersion stability of HRP molecules. Namely, HRP aggregates formed were dissociated to single molecules by weak inter-macromolecular interaction with the TNS, which was demonstrated by DLS measurements of the solution before and after the addition of TNS. In other words, the TNS act as surfactants for the HRP aggregates and an apparent HRP

concentration was increased. We believe that the “weak” interaction between HRP and TNS is derived from hydrogen bonds of surface hydroxyl groups of TNS and amino acid residues of HRP. However, the preferable effect of TNS could not occur in an acidic solution that caused a “firm” electrostatic interaction. In this case, formation of large aggregates with a disordered arrangement of HRP and TNS took place, and hence reduced an effective concentration of HRP. Moreover, the TNS addition realized for an improved enzymatic activity of superoxide dismutase (SOD). Such activity enhancement using the “weak” interaction should be extended to many other enzymes and functional proteins besides HRP and SOD. Therefore, further study of influence of TNS on catalytic activity of other enzymes is in progress.

Acknowledgements

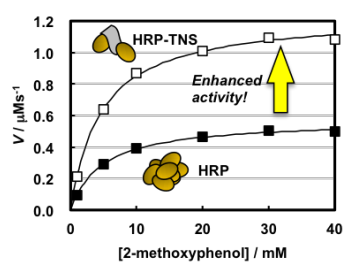
The present work was partly supported by JSPS KAKENHI Grant No. 26410244 and 15K05542.

Notes and references

- R. Voss, M.A. Brook, J. Thompson, Y. Chen, R.H. Pelton and J.D. Brennan, *J. Mater. Chem.*, 2007, **17**, 4854.
- K.M. Ho, X. Mao, L. Gu and P. Li, *Langmuir*, 2008, **24**, 11036.
- N. Soh, S. Kaneko, K. Uozumi, T. Ueda and K. Kamada, *J. Mater. Sci.*, 2014, **49**, 8010.
- V.K. Mudhivarthi, A. Bhambhani and C.V. Kumar, *Dalton Trans.*, 2007, 5483.
- A. Pattammattel, I.K. Deshapriya, R. Chowdhury and C.V. Kumar, *Langmuir*, 2013, **29**, 2971.
- R. Chowdhury, B. Stromer, B. Pokharel and C.V. Kumar, *Langmuir*, 2012, **28**, 11881.
- Y. Zhang, X. Chen, J. Wang and W. Yang, *Electrochem. Solid-State Lett.*, 2008, **11**, F19.
- C.V. Kumar and G.L. McLendon, *Chem. Mater.*, 1997, **9**, 863.
- Q. Wang Q. Gao and J. Shi, *J. Am. Chem. Soc.*, 2004, **126**, 14346.
- K. Kamada, S. Tsukahara and N. Soh, *J. Phys. Chem. C*, 2011, **115**, 13232.
- L. Zhang, Q. Zhang and J. Li, *Adv. Funct. Mater.*, 2007, **17**, 1958.
- J.C. Bretschneider, M. Reismann, G. Von Plessen and U. Simon, *Small*, 2009, **5**, 2549.
- L. Fruk, V. Rajendran, M. Spengler and C.M. Niemeyer, *ChemBioChem*, 2007, **8**, 2195.
- K. Kamada, T. Nakamura and S. Tsukahara, *Chem. Mater.*, 2011, **23**, 2968.
- M. Miljevic, B. Geiseler, T. Bergfeldt, P. Bockstaller and L. Fruk, *Adv. Funct. Mater.*, 2014, **24**, 907.
- Y. Zhang, L. Pang, C. Ma, Q. Tu, R. Zhang, E. Saeed, A.E. Mahmoud and J. Wang, *Anal. Chem.*, 2014, **86**, 3092.
- S. Kohse, A. Neubauer, A. Pazidis, S. Lochbrunner and U. Kragl, *J. Am. Chem. Soc.*, 2013, **135**, 9407.
- S. Kohse, A. Neubauer, S. Lochbrunner and U. Kragl, *ChemCatChem*, 2015, **6**, 3511.
- K. Kamada, S. Tsukahara and N. Soh, *J. Mater. Chem.*, 2010, **20**, 5646.
- C.V. Kumar and A. Chaudhari, *J. Am. Chem. Soc.*, 2000, **122**, 830.
- C.V. Kumar and A. Chaudhari, *Chem. Commun.*, 2002, 2382.
- H. Li, S. Guo, C. Li, H. Huang, Y. Liu and Z. Kang, *ACS Appl. Mater. Interfaces*, 2015, **7**, 10004.

- 23 H. Li, W. Kong, J. Liu, M. Yang, H. Huang, Y. Liu and Z. Kang, *J. Mater. Chem. B*, 2014, **2**, 5652.
- 24 T. Ohya, A. Nakayama, T. Ban, Y. Ohya and Y. Takahashi, *Chem. Mater.*, 2002, **14**, 3082.
- 25 K. Kamada and N. Soh, *RSC Adv.*, 2014, **4**, 8682.
- 26 M. Ragnar, C.T. Lindgren and N.-O. Nilvebrant, *J. Wood Chem. Technol.*, 2000, **20**, 277.
- 27 K. Kamada, *RSC Adv.*, 2014, **4**, 43052.
- 28 W. Ohashi, S. Inouye, T. Yamazaki and H. Hirota, *J. Biochem.*, 2005, **138**, 613.
- 29 K. Kamada and N. Soh, *J. Phys. Chem. B*, 2015, **119**, 5304.
- 30 C. Korsvik, S. Patil, S. Seal and W.T. Self, *Chem. Commun.*, 2007, 1056.

TOC graphic



Enzymatic activity of horseradish peroxidase (HRP) at diluted conditions is highly increased under the presence of nanometric titanate nanosheets (TNS).